Full Length Article

High-triplet-level phthalimide based acceptors for exciplexes with multicolor emission

Marian Chapran[a], Roman Lytvyn[b,c], Corentin Begel[b], Gabriela Wiosna-Salyga[a], Jacek Ulanski[a], Marharyta Vasylieva[d], Dmytro Volyniuk[b], Przemyslaw Data[d,e] and Juozas Vidas Grazulevicius[b*]

[a]Lodz University of Technology, Department of Molecular Physics, Zeromskiego 116, 90-924 Lodz, Poland
[b] Department of Polymer Chemistry and Technology, Kaunas University of Technology, Radvilenu Plentas 19, LT-50254 Kaunas, Lithuania
[c]Department of Organic Chemistry, Ivan Franko National University of Lviv, Kyryla i Mefodiya St. 6, Lviv 79005, Ukraine
[d]Faculty of Chemistry, Silesian University of Technology, M. Strzody 9, 44-100, Gliwice, Poland
[e]Department of Physics, Durham University, South Road, Durham DH1 3LE, United Kingdom

Keywords: exciplex, phthalimide, acceptors, thermally activated delayed fluorescence (TADF), organic light emitting diode (OLED)

Highlights:
- Five novel phthalimide based acceptors with high triplet levels (2.92-3.11 eV)
- Exciplex forming properties of acceptors were sensitive to the molecules design
- A para- substituted phthalimide-benzophenone in blend with carbazole containing donor showed sky-blue exciplex emission with small singlet-triplet splitting (0.06±0.03eV).

Abstract

To provide high exciton utilization in organic light emitting diodes, phthalimide derivatives were designed and synthesized as exciplex-forming materials. Due to high triplet levels (2.92-3.11 eV) and ionization potentials (7.18-7.29 eV), the developed phthalimide derivatives were found to be not only appropriate accepting materials for the formation of different color exciplexes but also as bifunctional materials with a satisfactory hole and exciton-blocking abilities. Solid-state blends of the synthesized phthalimides as acceptors and a carbazole containing donors showed exciplex emission. Bimolecular blends exhibited multicolor exciplex emission which covered a visible spectrum from sky-blue to red colors, depending on the donor used. However, the photoluminescence quantum efficiencies of the studied exciplex-forming systems were found to be sensitive to the molecular design of the phthalimides. Acceptor with para- substituted phthalimide showed better exciplex-forming properties in comparison to other compounds. Exciplex-forming blend of (2-(4-benzoylphenyl)isoindoline-1,3-dione) as an acceptor and 1,3-di(9H-carbazol-9-yl)benzene (mCP) as a donor showed the most efficient sky-blue emission with small singlet-triplet splitting (0.06±0.03eV). Such exciplex-forming molecular mixture was implemented as the light-emitting material in the sky-blue organic light emitting diodes which showed the

brightness of 2500 cd m^{-2} and maximum external quantum efficiency of 2.9 % due to the employment of both singlet and triplet excitons.

1. Introduction

Organic light emitting diodes (OLEDs) have attracted the attention due to their application in displays[1] and in solid-state lighting technology[2]. Organic molecules exhibiting thermally activated delayed fluorescence (TADF)[3] are of great interest due to their applications in OLEDs as efficient emitters and hosts[4]. Such devices can reach efficiency close to that of phosphorescent OLEDs. A key factor to generate efficient TADF is small singlet-triplet energy gap (ΔE_{ST} <kT)[5]. Chemical obstacles arising during synthesis of such type of molecules, often limit the realization of the TADF phenomenon via excited state of a single molecule[4].

As an alternative, TADF can be achieved by using emission from bimolecular excited species, in particular, exciplexes[6,7]. Such mechanism can operate in appropriately selected donor (D) and acceptor (A) fluorescent low molecular semiconductor systems, with the subsequent formation of excited intermolecular charge transfer (CT) complexes (exciplexes). An exciplex can be formed as a result of electron transfer from donor to acceptor molecules under Coulomb interactions[8]. In such systems, HOMO and LUMO energy orbitals are separated by a relatively long distance leading to small exchange energy and efficient reverse intersystem crossing (RISC) process from the triplet excited state to the singlet one. Owing to harvesting of dark triplets excitons internal quantum efficiency close to 100% can be achieved[9]. Bimolecular charge-transfer (CT) systems (exciplexes) find application in white electroluminescence devices either as emitters due to broad emission spectrum[10,11,12] or as hosts for fluorescent, phosphorescent or TADF dopants[13,12]. Employing exciplex forming pair as a host in OLEDs provided good operation stability and long lifetime of devices as a result of charge carrier balance in OLED structure[14]. Moreover, multicolor OLEDs can be designed using efficient exciplex-forming systems with one acceptor and several donors to achieve simultaneously multicolor luminescence and efficient triplet harvesting[10]. However, application of exciplex-forming systems as emitters is still challenging due to the difficulties in developing of efficient CT systems with high photoluminescence (PL) and electroluminescence (EL) yields[7]. To obtain TADF the charge-transfer singlet (^{1}CT) and the charge-transfer triplet (^{3}CT) states of exciplexes should lie lower or close to the triplet levels of the corresponding exciplex forming units.[15,16 ,17]. A progress in the field of high-efficiency exciplex emission based OLEDs can be reached by the design and synthesis of new suitable electron donating and electron accepting molecules with high triplet levels. Different types of compounds were tested as the electron donating units, among them triphenylamine and a carbazole containing derivatives due to their good electronic and optical properties and commercial availability[4]. Also numerous accepting molecules were developed as the electron accepting counterparts such as derivatives of triazine, phthalimide, benzimidazole, oxadiazole, pyridine[18,19].

One of the well-known accepting unit is phthalimide moiety, derivatives of which are used as synthetic precursors for the synthesis of organic semiconductors. Phthalimide derivatives have found applications in optoelectronic and electronic devices such as solar cells[20,21], organic thin-film transistors[22,23] and organic light emitting diodes[24,25]. The main advantages of phthalimides are cheap and simple synthetic synthesis, strong accepting properties (low lying LUMO levels), high triplet energy levels and high thermal stability[20,25,26]. Recently application of phthalimide moiety as the acceptor building block in TADF molecules was reported[27,28,29]. However, to our best knowledge, exciplex-forming properties of phthalimide containing materials have not been studied yet.

In this work, we unclosed potential of phthalimide derivatives as accepting exciplex-forming materials for OLEDs application and studied the effect their molecular structure modifications on exciplex emission efficiency. Five new phthalimide derivatives 2,2'-(oxybis(4,1-phenylene))bis(isoindoline-1,3-dione)(**DPOPht$_2$**), 2,2'-(pentane-1,5-diylbis(4,1-phenylene))bis(isoindoline-1,3-dione) (**CyPh$_2$Pht$_2$**), 2-(2-benzoylphenyl)isoindoline-1,3-dione (**2-BpPht**), 2-(3-benzoylphenyl)isoindoline-1,3-dione (**3-BpPht**), 2-(4-benzoylphenyl)isoindoline-1,3-dione (**4-BpPht**) (**Figure 1**) were designed, synthesized and characterized.

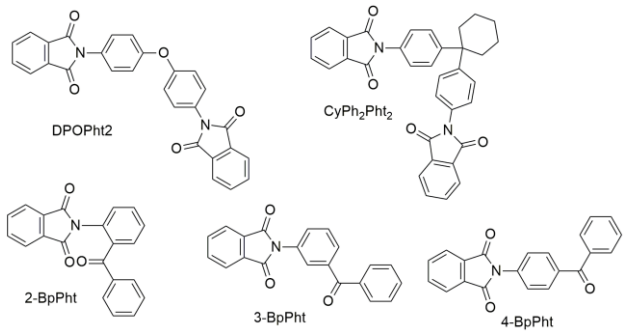

Figure 1. Chemical structures of the studied new phthalimide derivatives: DPOPht$_2$, CyPh$_2$Pht$_2$, 2-BpPht, 3-BpPht and 4-BpPht

Theoretical investigations by means of density functional theory (DFT) were performed to determine the geometry and HOMO and LUMO distribution of the synthesized compounds. Their photophysical properties were studied to elucidate exciplex-forming ability. All phthalimide derivatives showed high triplet levels and low-lying HOMO levels. Moreover, using **DPOPht$_2$**, **CyPh$_2$Pht$_2$, 2-BpPht, 3-BpPht, 4-BpPht** acceptors and 1,3-di(9H-carbazol-9-yl)benzene (mCP), 4,4′-bis(N-carbazolyl)-1,1′-biphenyl (CBP), poly(9-vinylcarbazole) (PVK), tris(4-carbazoyl-9-ylphenyl)amine (TCTA) as electron donors, different exciplex-forming systems emitting in sky-blue, green and red regions were developed. The detailed steady-state and time-resolved spectroscopic studies were carried out to disclose the benefits of the current design strategy of efficient exciplex-forming acceptors.

2. Experimental section

2.1. Materials. All reactions do not require special precautions (excluding moisture influence) and were performed under air atmosphere. Dry solvents and all the other reagents were purchased from Sigma Aldrich or Alfa Aesar and used without further purification.

General procedure for the synthesis of phthalimide acceptors

An equimolecular mixture of phthalic anhydride (5 mmol) and corresponding amine (5 mmol) (in case of compounds $DPOPht_2$ and $CyPh_2Pht_2$ the ratio of reagents were 2:1) were stirred under refluxing in glacial acetic acid (35 ml) during 12 hr. Then acetic anhydride (15 ml) was added in one portion and mixture was stirred under refluxing for additional 5 hr. The cold reaction mixture was poured into distilled water (150 ml). Precipitated sediment was filtered off and washed several times with distilled water. The obtained crude material was recrystallized from i-PrOH/DMF mixture of solvents.

2,2'-[Oxybis(4,1-phenylene)]bis(1H-isoindole-1,3(2H)-dione) $DPOPht_2$

White crystals, yield 70 %, mp 289-290°C (mp 291°C[30]). ^{1}H NMR (250 MHz, $CDCl_3$), δ: 7.98 – 7.93 (m, 4H), 7.83 – 7.77 (m, 4H), 7.44 (dt, *J* = 9.0, 2.3 Hz, 4H), 7.20 (dt, *J* = 9.0, 2.3 Hz, 4H). ^{13}C NMR (175 MHz, $CDCl_3$), δ: 167.37, 156.46, 134.47, 131.79, 128.21, 127.07, 123.81, 119.56. MS (MALDI-TOF) m/z $[M]^-$ calcd for $C_{28}H_{16}N_2O_5$: 460.45; found, 460.65. Elemental analysis cal. for $C_{28}H_{16}N_2O_5$ C, 73.04; H, 3.50; N, 6.08. Found (%): C, 73.25; H, 3.61; N, 6.13.

2,2'-[Cyclohexane-1,1-diylbis(4,1-phenylene)]bis(1H-isoindole-1,3(2H)-dione) $CyPh_2Pht_2$

Off-white crystals, yield 54 %, mp 283-284°C ^{1}H NMR (250 MHz, $CDCl_3$), δ: 8.00 – 7.91 (m, 4H), 7.83 – 7.74 (m, 4H), 7.45 (dt, *J* = 9.0, 2.3 Hz, 4H), 7.38 (dt, *J* = 9.0, 2.3 Hz, 4H), 2.38 – 2.31 (m, 4H), 1.66 – 1.49 (m, 6H). ^{13}C NMR (175 MHz, $CDCl_3$), δ: 167.35, 147.95, 134.35, 131.85, 129.20, 128.04, 126.11, 123.74, 46.26, 37.24, 26.30, 22.85. MS (MALDI-TOF) m/z $[M+K]^-$ calcd for $C_{34}H_{26}N_2O_4$: 565.70; found, 565.75 Elemental analysis cal. for $C_{34}H_{26}N_2O_4$ C, 77.55; H, 4.98; N, 5.32. Found (%): C, 77.69; H, 4.65; N, 5.42.

2-(2-Benzoylphenyl)-1H-isoindole-1,3(2H)-dione 2-BpPht

White crystals, yield 68 %, mp 198-199°C (mp 198-199°C[30]). ^{1}H NMR (250 MHz, $CDCl_3$) δ 7.85 – 7.63 (m, 8H), 7.58 – 7.30 (m, 5H). ^{13}C NMR (175 MHz, $CDCl_3$), δ: 195.22, 167.14, 137.12, 136.07, 134.28, 132.78, 132.04, 131.72, 130.87, 130.54, 129.91, 129.33, 128.33, 128.22, 123.72. MS (MALDI-TOF) m/z [M+H]- calcd for $C_{21}H_{14}NO_3$: 328.35; found, 328.51. Elemental analysis cal. for $C_{21}H_{13}NO_3$: C, 77.05; H, 4.00; N, 4.28. Found (%): C, 77.17; H, 4.09; N, 4.37.

2-(3-Benzoylphenyl)-1H-isoindole-1,3(2H)-dione 3-BpPht

White crystals, yield 76 %, mp 179-180°C (mp 177-179°C[30]). ^{1}H NMR (250 MHz, $CDCl_3$), δ: 8.01 – 7.93 (m, 2H), 7.93 – 7.84 (m, 4H), 7.84 – 7.77 (m, 2H), 7.74 – 7.63 (m, 2H), 7.59 (dt, *J* = 6.2, 1.4 Hz, 1H), 7.55 – 7.47 (m, 2H). ^{13}C NMR (175 MHz, $CDCl_3$) δ 195.42, 167.00, 138.47, 137.17, 134.63, 132.72, 131.80, 131.67, 130.25, 130.19, 129.46, 129.25, 128.45, 128.23, 123.93. MS (MALDI-TOF) m/z $[M+H]^-$ calcd for $C_{21}H_{14}NO_3$:

328.35; found, 328.55. Elemental analysis cal. for $C_{21}H_{13}NO_3$: C, 77.05; H, 4.00; N, 4.28. Found (%):C , 77.20; H, 4.11; N, 4.23.

2-(4-Benzoylphenyl)-1H-isoindole-1,3(2H)-dione 4-BpPht

White crystals, yield 72 %, mp 182-183°C (mp 183°C[30]). ^{1}H NMR (250 MHz, $CDCl_3$), δ: 8.02 – 7.92 (m, 4H), 7.88 – 7.80 (m, 4H), 7.69 – 7.57 (m, 3H), 7.56 – 7.46 (m, 2H). ^{13}C NMR (175 MHz, $CDCl_3$), δ: 195.68, 166.88, 137.40, 136.69, 135.45, 134.73, 132.64, 131.65, 130.89, 130.09, 128.42, 125.91, 124.01. MS (MALDI-TOF) m/z $[M+H]^-$ calcd for $C_{21}H_{14}NO_3$: 328.35; found, 328.51. Elemental analysis cal. for $C_{21}H_{13}NO_3$: C, 77.05; H, 4.00; N, 4.28. Found (%): C, 77.15; H, 4.07; N, 4.17.

2.2. Methods. ^{1}H spectra were recorded on a Bruker 250 MHz NMR spectrometer and ^{13}C NMR spectra were recorded on a Bruker Ultra Shield 700 MHz NMR spectrometer using $CDCl_3$ as the solvent. Chemical shifts (δ) are reported in ppm referenced to tetramethylsilane (TMS) as internal reference and coupling constants (J) in Hz. Melting points were measured using the Electrothermal MEL-TEMP melting point apparatus. The target compounds were characterized by matrix-assisted laser desorption/ionisation time-of-flight (MALDI-TOF) using an Axima-Performance TOF spectrometer (Shimadzu Biotech, Manchester, UK), equipped with a nitrogen laser (337 nm). The pulsed extraction ion source accelerated the ions to a kinetic energy of 20 keV. Elemental analysis was performed on an Exeter Analytical CE-440 elemental analyser.

2.3. Electrochemistry. Electrochemical measurements of 1.0 mM concentrations of phthalimide derivatives were conducted in 0.1 M tetrabutylammonium hexafluorophosphate (Bu_4NPF_6) (99%, Sigma Aldrich, dried) as the electrolyte and in dichloromethane (CHROMASOLV®, 99.9% Sigma Aldrich) as the solvent. All solutions were degassed using argon before measurement. The electrochemical cell comprised: platinum electrode with a 1 mm diameter of working area as a working electrode, an Ag/AgCl electrode as a reference electrode and a platinum coil as an auxiliary electrode. Cyclic voltammetry measurements were conducted at room temperature with a scan rate of 50 mV s^{-1} were calibrated with a ferrocene/ferrocenium redox couple. Electron affinity (E_A) was calculated from reduction (E_{red}) potential, respectively, using following equation: $E_A = E_{red} + 5.1$[31,32].

2.4. Photophysics. Absorption spectra were recorded with a Carry 5000 (Varian) spectrometer. Photoluminescence spectra of thin films and solutions were performed at room temperature with an Edinburgh Instruments FLS980 fluorescence spectrometer with Xe-lamp as an excitation source and R-928 photomultiplier detector. The photoluminescence quantum yields (PLQY) of the blends were measured using a calibrated integrating sphere from Edinburgh Instruments. Phosphorescence, prompt fluorescence (PF), and delayed fluorescence (DF) spectra and decays were acquired using nanosecond gated luminescence and lifetime measurements (from 400 ps to 1 s) using either a high energy pulsed Nd:YAG laser emitting at 355 nm (EKSPLA) or a N_2 laser emitting at 337 nm. Sample emission was focused onto a spectrograph and gated iCCD camera (Stanford Computer Optics). PF/DF time-resolved

measurements were performed by exponentially increasing gate and integration times. Low-temperature measurements were conducted using a liquid nitrogen cryostat (Janis Research) under a nitrogen atmosphere.

2.5. Devices. OLEDs have been fabricated on pre-cleaned, patterned indium-tin-oxide (ITO) coated glass substrates with a sheet resistance of 20 Ω/sq and ITO thickness of 100 nm. All small molecules and cathode layers were thermally evaporated in Kurt J. Lesker Spectros II evaporation system under pressure of 10^{-6} mbar without breaking the vacuum. The sizes of the pixels were 8 mm^2 and 16 mm^2. NPB (*N*,*N*′-di(1-naphthyl)-*N*,*N*′-diphenyl-(1,1′-biphenyl)-4,4′-diamine), TCTA (Tris(4-carbazoyl-9-ylphenyl)amine) were used as a Hole Injection Layer (HIL) and Hole Transport Layer (HTL), respectively. TmPyPB (3,3'-(5'-(3-(pyridin-3-yl)phenyl)-[1,1':3',1''-terphenyl]-3,3''-diyl)dipyridine) was introduced as a Hole Blocking Layer (HBL) and Electron Transport Layer (ETL). Lithium fluoride (LiF) and aluminium were used as the cathode. Organic semiconductors and aluminium were deposited at a rate of 1 $Å s^{-1}$, and the LiF layer was deposited at 0.1 $Å s^{-1}$. The characteristics of the devices were recorded using 10-inch integrating sphere (Labsphere) connected to a Source Meter Unit and Ocean Optics USB4000 spectrometer. All materials were purchased from Sigma Aldrich or Lumtec and were purified by temperature-gradient sublimation in a vacuum.

3. Results and discussion

3.1. Synthesis

Exciplex-forming acceptors were obtained in high yields by the simple one-pot condensation reaction of phthalic anhydride with commercially available amines (**Figure 2**). The compounds were obtained as white crystals, with good solubility in polar organic solvents (e.g., dichloromethane, chloroform, tetrahydrofuran). The synthesized compounds were characterized by ^{1}H, ^{13}C NMR spectroscopy, MALDI-TOF mass spectrometry and elemental analysis (details are described in the Supporting Information). Isomeric benzophenone containing compounds (**2-BpPht**, **3-BpPht**, **4-BpPht**) were prepared in order to check the influence of substitution pattern on electro-optical and exciplex-forming properties. On the other hand, disubstituted compounds with symmetric structure (**DPOPht$_2$**, **CyPh$_2$Pht$_2$**) were designed to increase the number of phthalimide groups per molecule.

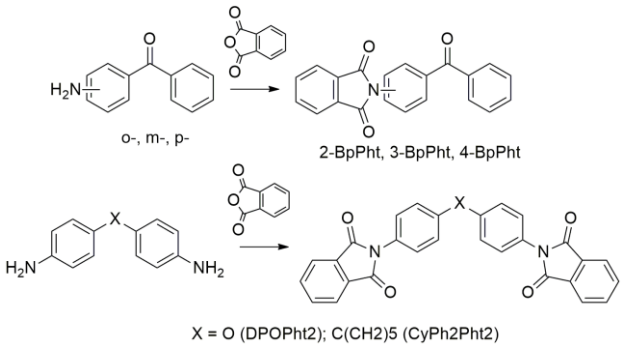

Figure 2. Synthesis of **2-BpPht**, **3-BpPht**, **4-BpPht**, **DPOPht$_2$**, **CyPh$_2$Pht$_2$**

3.2. Theoretical calculations

To analyze the geometry and the values of energies of the highest occupied molecular orbital (HOMO) and the lowest unoccupied molecular orbital (LUMO) quantum chemical calculations were performed for the molecules designed using density functional theory (DFT). All the calculations were performed with the software package Gaussian09 (Revision A.02)[33] with B3LYP/6-311G(d,p) level of theory.

The geometries of the molecules determined theoretically are presented in **Figure 3**. Different linkage topologies of the developed phthalimide derivatives result in different molecular structures from very twisted in the case of **2-BpPht** to completely liner in the case of **4-BpPht** (**Figure 3**, **Figure S11**). The theoretical HOMO and LUMO energy values of compounds are given in Table 1. For almost all the molecules LUMO orbitals predominantly are located on phthalimide structural units, while HOMO frontier orbitals are located on N-aryl substituents. For compound **2-BpPht** due to orto-substitution of benzophenone and phthalimide moieties, LUMO orbitals are located on phthalimide and closely situated benzoyl unit of benzophenone moieties, while HOMO is located on phthalimide and N-phenyl units. For all the synthesized compounds LUMO values are in the range of 2.4-2.6 eV, proving their strong accepting properties.

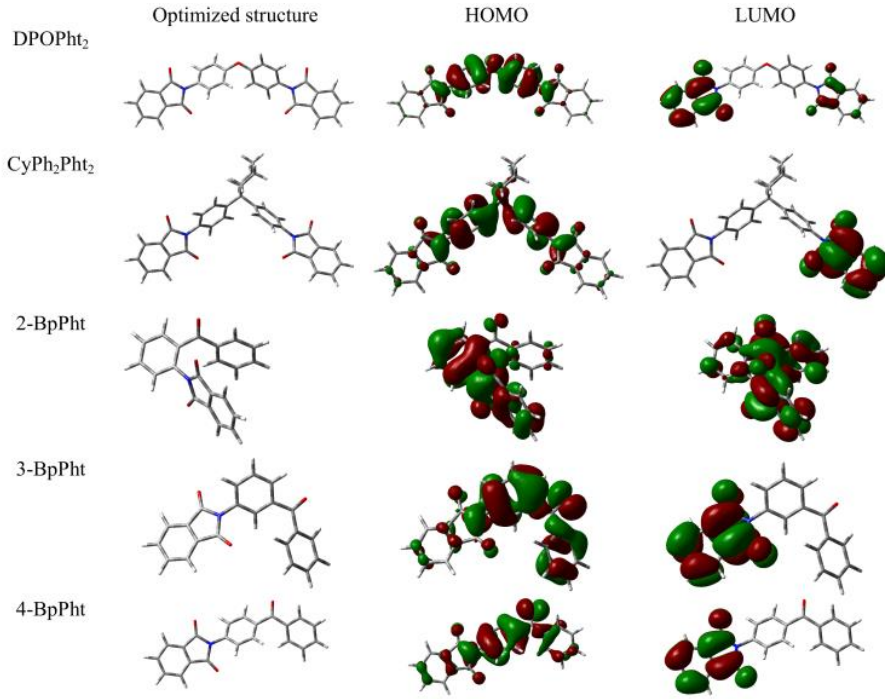

Figure 3. Fully optimized structures of studied phthalimide derivatives and graphical representation of the HOMO and LUMO calculated at the B3LYP/6-311G (d,p) level of theory.

3.3. Photophysical properties

The normalized optical absorption spectra of the dilute solutions and thin films of the acceptors are shown in **Figure 4**. Three main regions can be identified in the absorption spectra: the lower-energy bands in the range of 275–310 nm, and the higher-energy bands in the ranges of 240-260 nm and 200–250 nm.

The higher energy absorption band corresponds to n-π* transition and the lower energy absorption band is related to the main π-π* transition[34]. The observed absorption spectrum originated mainly from the N-aryl-substituted phthalimide moieties. Absorption maxima of the phthalimide derivatives of the thin films are slightly red-shifted in comparison to those of dilute solutions. Such a shift can be attributed to the intermolecular interactions between molecules that are more likely to occur in the solid state[35]. The optical band gaps E_g were estimated from the longest wavelength absorption edge of the UV−VIS spectra. The E_g values are given in **Table 1**. **4-BpPht** showed the longest wavelength absorption centered at 280 nm, with higher intensity than the other acceptors. This observation can be explained by more effective conjugation in this para-substituted phthalimide derivative.

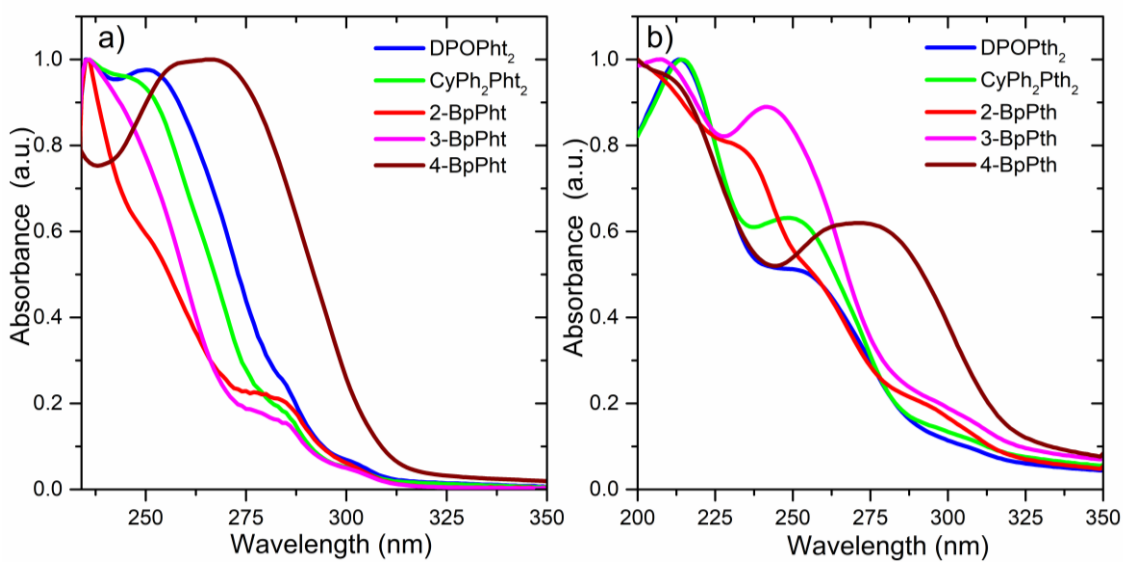

Figure 4. UV-VIS absorption spectra of the dilute solutions (10^{-5} M in THF) (a) and of spin-coated thin layers (b) of the synthesized phthalimide derivatives.

Photoluminescence spectra (**Figure 5**) revealed the main band, with a small Stokes shift, centered at 305 nm. Fluorescence bands of all the molecules studied have very similar shapes with an identical position of maximum intensity. This observation indicates that the main transitions originate from phthalimide moiety. PL spectra of neat films of **DPOPht2**, **CyPh2Pht2**, **2-BpPht**, **3-BpPht** and **4-BpPht** were not analysed due to a very weak photoluminescence. One of the crucial parameters of exciplex forming acceptor is relatively high triplet levels where locally excited states of donor or acceptor (^3LE_D or ^3LE_A) lie close to the ^1CT of exciplex or visibly stay above the ^1CT because of efficient RISC[36,37,38] Molecules **2-BpPht**, **3-BpPht**, **4-BpPht** showed similarly structured (with 5 peaks) phosphorescence which can be assigned to the ^3LE triplet emission. On another hand, two symmetric molecules **DPOPht2** and **CyPh2Pht2** exhibited broad, not structured CT phosphorescence (**Figure 5b**). The values of triplet levels were estimated from the onsets of phosphorescence spectra (**Table 2**). The substituents attached at orto-, meta- and para-positions of benzophenone moiety in **2-BpPht**, **3-BpPht**, **4-BpPht**, respectively, do not have any substantial influence on the phosphorescence and all triplet levels were found to be

around 3.1eV. The onset of phosphorescence emission of **4-BpPht** was slightly red-shifted in comparison to those of other two benzophenone phthalimide acceptors. Symmetric phthalimide acceptors **DPOPht2** and **CyPh2Pht2** exhibited triplet levels at 2.98 and 2.92 eV which are slightly lower than those of **2-BpPht**, **3-BpPht**, **4-BpPht**. This effect can be explained by the presence of additional phthalimide moiety.

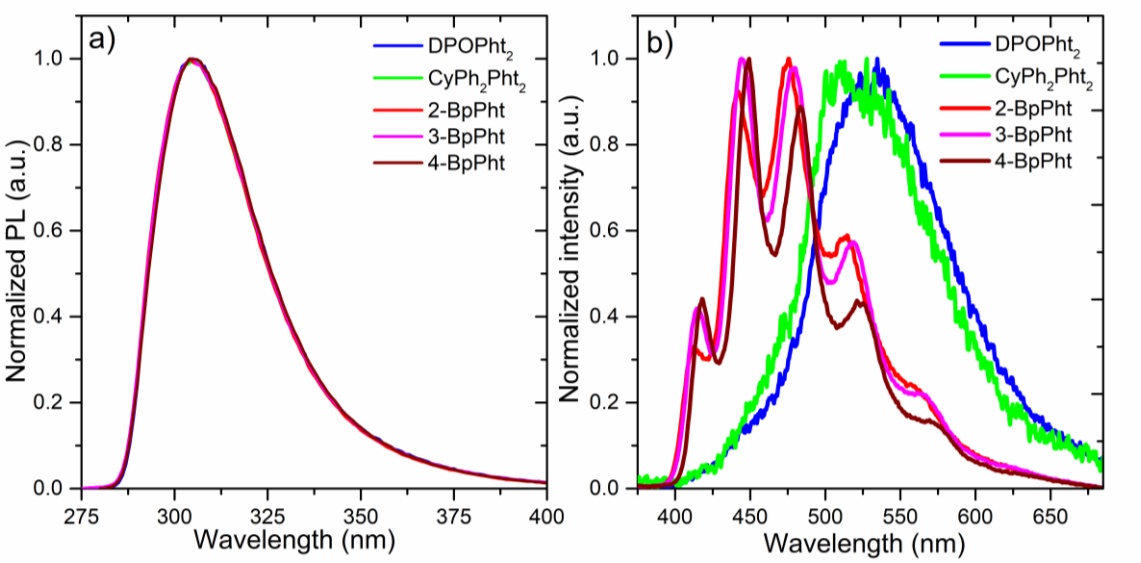

Figure 5. Photoluminescence spectra of THF solutions (10^{-5}M) of the phthalimide derivatives (a) and phosphorescence spectra of their molecular dispersions in the zeonex matrix at 80K (b).

3.4. Electrochemical properties

Electrochemical properties of the solutions of the synthesized phthalimide derivatives in dichloromethane (DCM) with 0.1 M tetrabutylammonium hexafluorophosphate as the electrolyte were studied by cyclic voltammetry (CV). The CV curves of compounds are shown in **Figure 6**. The curves had similar shapes, and the compounds exhibited close reduction potentials, and as a consequence comparable values of electron affinity (E_A). (**Table 1**). All the compounds were characterized by the reversible one-electron process. The positions of the main peaks of CV curves (**Figure 6a**) were conditioned by reduction of phthalimide group, and small shifts were related to the different substituents. The position of the second peak (the second step of reduction) (**Figure 6b**) was found to be close to the limit of the scanning range, which was restricted due to the solvent (DCM) instability within the negative potential range. Non-halogenated solvents could not be used due to poor solubility of the compounds. **DPOPht2**, **CyPh2Pht2** as well as **3-BpPht** and **4-BpPht** showed the similar positions of the 2nd peaks of reduction. These peaks corresponded to the reduction of phthalimide and benzophenone groups[39,40]. Small differences between positions of peaks can be attributed to the different environment of redox groups. Two parts of **CyPh2Pht2** are linked by a non-conjugated bridge and therefore behave as separate species. The absence of the 2nd peak in the CV curve of compound **2-BpPht** can apparently be explained by the steric

effect. Oxidation peaks were not observed in the CV curves, and consequently, the ionization potentials (I_P) were estimated using the UV-Vis spectroscopic data.

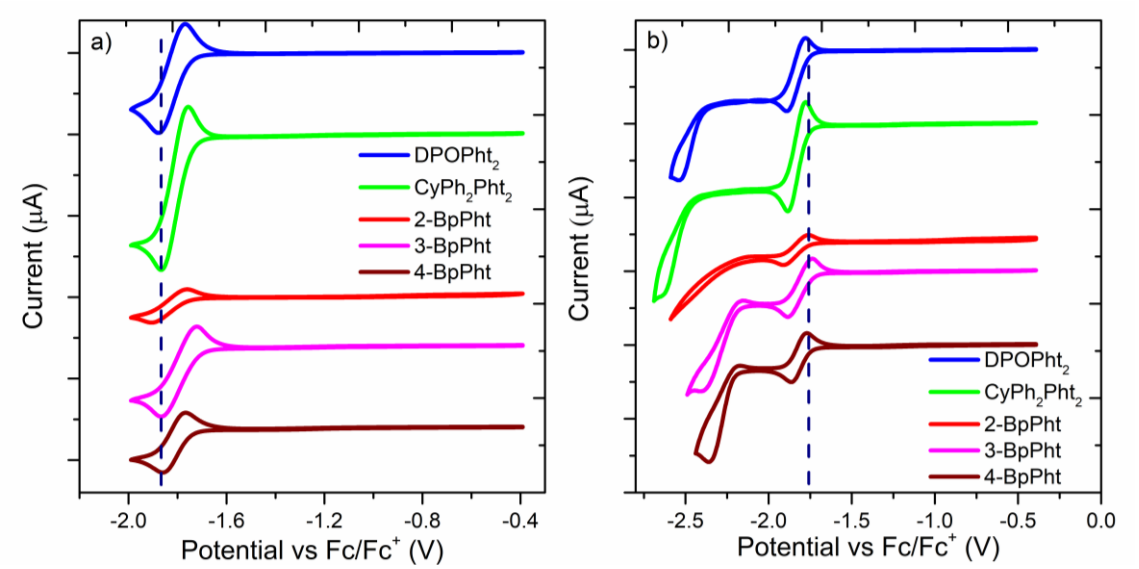

Figure 6. CV curves of phthalimide derivatives with the first (a) and the second (b) steps of reduction.

Table 1. Summary of electrochemical and optical data

	Eg[1], eV	E_{red} [2] vs E_{ferro}, V	E_A [3], eV	I_P [4], eV	LUMO[5], eV	HOMO[5], eV	T_1 [6], eV
$DPOPht_2$	3.84	-1.73	3.37	7.21	-2.48	-6.02	2.98
$CyPh_2Pht_2$	3.91	-1.74	3.36	7.27	-2.42	-6.20	2.92
2-BpPht	3.83	-1.75	3.35	7.18	-2.52	-6.85	3.12
3-BpPht	3.89	-1.7	3.40	7.29	-2.64	-6.82	3.11
4-BpPht	3.90	-1.73	3.37	7.27	-2.64	-6.73	3.08

[1]Optical band gap estimated from the edges of electronic absorption spectra

[2]E_{red} are measured vs. ferrocene/ferrocenium

[3]Electron affinities measured by the electrochemical method

[4]Ionization potentials calculated from the band gap: $I_P = E_A + E_g$

[5]HOMO and LUMO energies calculated at the B3LYP/6-311G (d,p) level "in a vacuum".

[6]T_1 calculated from onset of phosphorescence spectra

3.5. Exciplex-forming properties

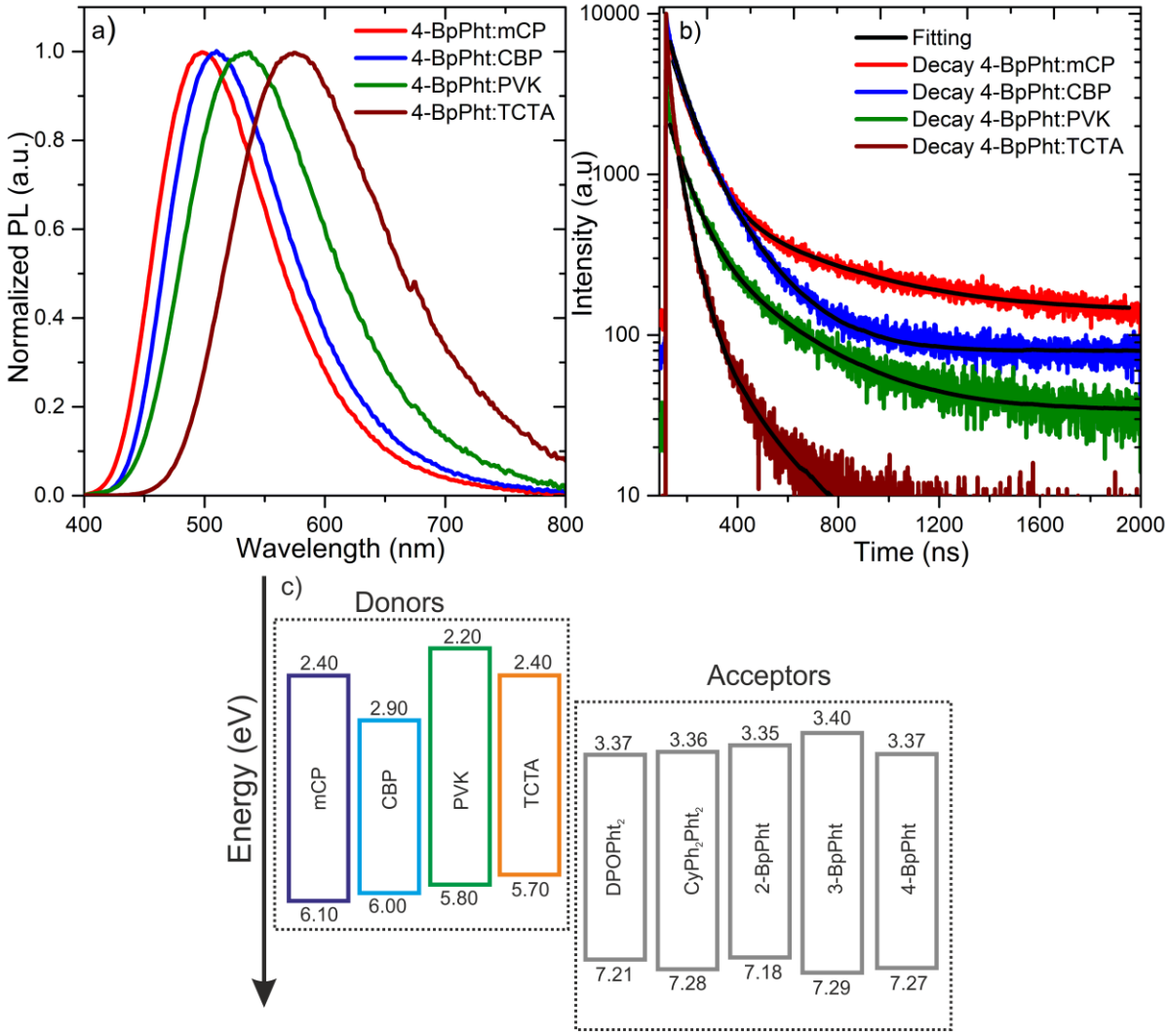

Figure 7. PL spectra (a) and PL decay curves (b) of the blends layers: 4-BpPht:mCP, 4-BpPht:CBP, 4-BpPht:PVK and 4-BpPht:TCTA. Schematic representation of energy band diagrams of carbazole-based donors and phthalimide acceptors for exciplex emissions (c).

The main advantages of phthalimide acceptors are exciplex-forming properties which have been detected for solid-state samples of molecular mixtures with carbazole-containing donors such as 1,3-bis(N-carbazolyl)benzene (mCP), 4,4′-bis(N-carbazolyl)-1,1′-biphenyl (CBP), tris(4-carbazoyl-9-ylphenyl)amine (TCTA) and poly(9-vynylcarbazole) (PVK). The molecular mixtures formed with weight ratio 1:1 of all the synthesized materials with appropriate donors showed emission bands red shifted in comparison with either the donor or acceptor pristine emission spectra, and such broad Gaussian-type emission bands are typical for exciplexes (**Figure S12**)[8,41,42]. **Figure 7a** (as well as **Figure S13** and **Figure S14**) show PL spectra of exciplex-forming blends containing phthalimide acceptors and mCP, CBP, PVK and TCTA as donors. The acceptors have the similar electron affinity (E_A) values in the range 3.3-3.4 eV and exhibit sky-blue emission with mCP (I_p=6.1 eV), blue-greenish emission with CBP (I_p=6.0 eV), green emission with PVK (I_p=5.8 eV) and orange emission

with TCTA (I_p=5.7 eV) (**Figure 7c**). Such colour tuning can be explained by CT exciplex emission which is a function of the difference between ionization potential (I_P) of donors and electron affinity (E_A) of accepting molecules.[42,43,44]. This is one of the advantages of exciplex emission. By selection of appropriate materials (donor or acceptor), CT emission can be tuned. Such bimolecular exciplex-forming materials can be adopted in OLEDs for emissive layers or as hosts for a wide range of phosphorescent or TADF emitters.

Considering the exciplex-forming properties, the PL decay dynamics and the photoluminescence quantum efficiencies (PLQY) of all twenty exciplex-forming systems were characterized at room temperature (**Table 2**, **Figure S13**). The PL decay curves showed biexpotential character. The life times (τ_1, τ_2) of the layers as well as the PLQY values of the mixtures are given in **Table 2**. The exciplex-forming blends of studied compounds with mCP exhibited sky blue emission with a maximum peak in the range of 494-497 nm (**Figure S13**, **Figure S14**). The mCP:**DPOPht$_2$** and mCP:**CyPh$_2$Pht$_2$** exciplexes exhibited low PLQY of 0.8% and 2 % respectively, and short-lived prompt (τ_1 = 30 – 40 ns) and delayed emission (τ_2 = ca.140ns). Bimolecular blends mCP:**2-BpPht**, mCP:**3-BpPht**, mCP:**4-BpPht** exhibited much higher PLQY values of 18%, 20% and 26% respectively with longer decay times equal around 80 ns (τ_1) and 420 ns (τ_2) in comparison with mCP:**DPOPht$_2$** and mCP:**CyPh$_2$Pht$_2$** exciplexes. Bimolecular blends with CBP as a donor showed emission with a maximum peak in the range of 504-510 nm (**Figure S13**, **Figure S14**). The values of PLQY were found to be 1.6% for CBP:**DPOPht$_2$**, 4% for CBP: **CyPh$_2$Pht$_2$**, 17% for CBP:**2-BpPht**, 19% CBP:**3-BpPht** and 22% for CBP:**4-BpPht**. The lifetimes (τ_1, τ_2) of the emission of the exciplexes based on **2-BpPht**, **3-BpPht** and **4-BpPht** were found to be longer than those observed for the exciplexes based on symmetric acceptors (**DPOPht$_2$**, **CyPh$_2$Pht$_2$**). Bimolecular excited states of the molecular mixtures containing PVK displayed fluorescence maxima at 530-540 nm, i.e. in the green part of the visible spectrum. Photoluminescence quantum yield of thin films were found to be 2.5% and 3% for PVK:**DPOPht$_2$** and PVK:**CyPh$_2$Pht$_2$** exciplexes, respectively. **2-BpPht**, **3-BpPht** and **4-BpPht** dispersed in PVK showed slightly higher values of PLQY: 6%, 6% and 8%, respectively. PL decays of the blends with PVK showed similar behavior, but a longer-lived component of PVK:**2-BpPht**, PVK:**3-BpPht** and PVK:**4-BpPht** exhibited twice longer emission lifetime than the molecular mixtures of PVK with another acceptor studied (**Figure S13**, **Figure S14**). Indeed, the blends with PVK as a donor showed less efficient exciplex emission than the molecular mixtures with mCP and CBP. This observation can be explained by the weak interaction between the acceptor molecules and the carbazole units of the polymer due to longer distance between the donor and the acceptor molecules. The last group of materials exhibiting lower energy exciplex emission contain TCTA as a donor. They emit light in an orange part of the spectrum with peaks at 565-575 nm (**Figure S13**, **Figure S14**). The solid films of the systems containing TCTA showed low PLQY of exciplex emission. Taking all these observations into account, one can predict, that introducing of stronger accepting (with lower HOMO) connectors between the phthalimide units should prevent the formation of low energy intramolecular CT-state. As a result, significant enhancement of photophysical and exciplex forming properties could be expected.

The results described above show that the compounds with phthalimide moiety attached to orto-, meta- and para position of benzophenone moiety exhibit good exciplex-forming properties, and in particular the para isomer **4-BpPht**. This compound in combination with mCP forms exciplex with PLQY of 26 %, the highest observed in this work.

Table 2. Photopysical propreties of exciplex-forming blends

Eciplexes	PL λ_{max} (nm)	PLQY (%)	τ_1 ns (%)	τ_2 ns (%)	χ^2
mCP:DPOPht$_2$	498	0.8	38.1 (65)	138.9 (35)	1.23
mCP:CyPh$_2$Pht$_2$	496	2	36.8 (69)	145.8 (31)	1.28
mCP:2-BpPht	494	18	82.5 (53)	420.6 (47)	1.28
mCP:3-BpPht	495	20	80.3 (66)	420.2 (34)	1.23
mCP:4-BpPht	497	26	77.5 (63)	418.9 (37)	1.28
CBP:DPOPht$_2$	510	1.6	24.1 (56)	98.1 (44)	1.25
CBP:CyPh$_2$Pht$_2$	503	4	40.3 (71)	131.9 (29)	1.25
CBP:2-BpPht	504	17	63.6 (44)	193.9 (56)	1.15
CBP:3-BpPht	503	19	64.3 (52)	178.3 (48)	1.17
CBP:4-BpPht	510	22	64.1 (49)	173.5 (51)	1.13
PVK:DPOPht$_2$	540	2.5	54.1 (59)	204.7 (41)	1.25
PVK:CyPh$_2$Pht$_2$	530	3	69.7 (59)	255.9 (41)	1.19
PVK:2-BpPht	525	6	86.1 (38)	348.1 (62)	1.07
PVK:3-BpPht	528	6	99.2 (58)	389.4 (42)	1.22
PVK:4-BpPht	533	8	71.2 (54)	291.7 (46)	1.20
TCTA:DPOPht$_2$	570	2	34.4 (84)	123.9 (16)	1.22
TCTA:CyPh$_2$Pht$_2$	566	2	43.1 (79)	143.2 (21)	1.27
TCTA:2-BpPht	569	2	65.1 (79)	226.5 (21)	1.18
TCTA:3-BpPht	563	3	45.6 (79)	170.9 (21)	1.27
TCTA:4-BpPht	575	5	45.8 (83)	184.1 (17)	1.29

In general, photophysics of exciplex-forming systems is more complex than that of individual compounds exhibiting intramolecular CT. We have noticed, that the biexponential PL decay curves with short- and long-lived components are characteristic of the studied molecular mixtures. Long-lived components can be of different origin and require deeper investigations. To characterize the exciplex between mCP and **4-BpPht** and to study the driving mechanisms of it, the time-resolved PL measurements have been performed.

Figure 8a shows PL decay of mCP:**4-BpPht** recorded at 295K and 80K. At both temperatures, the PL decays of the blend related to the short-lived prompt fluorescence and the long-lived TADF clearly follow exponential decay laws. Delayed emission of bimolecular CT at 80K showed longer lifetime (up to 100 ms), than at room temperature (up to 200 μs) which is typical behavior for the TADF materials. This observation is consistent with the fact that at high temperature due to thermal activation the RISC become more efficient causing shorter-lived delayed emission[9]. To confirm the TADF exciplex mechanism, the

dependence of the delayed fluorescence intensity vs laser pulse energy was plotted (**Figure 8d**). The linear relationship with the slope close to 1 (0.89) confirms that the delayed fluorescent mechanism in the studied exciplex is dominated by TADF process rather than by triplet-triplet annihilation[45].

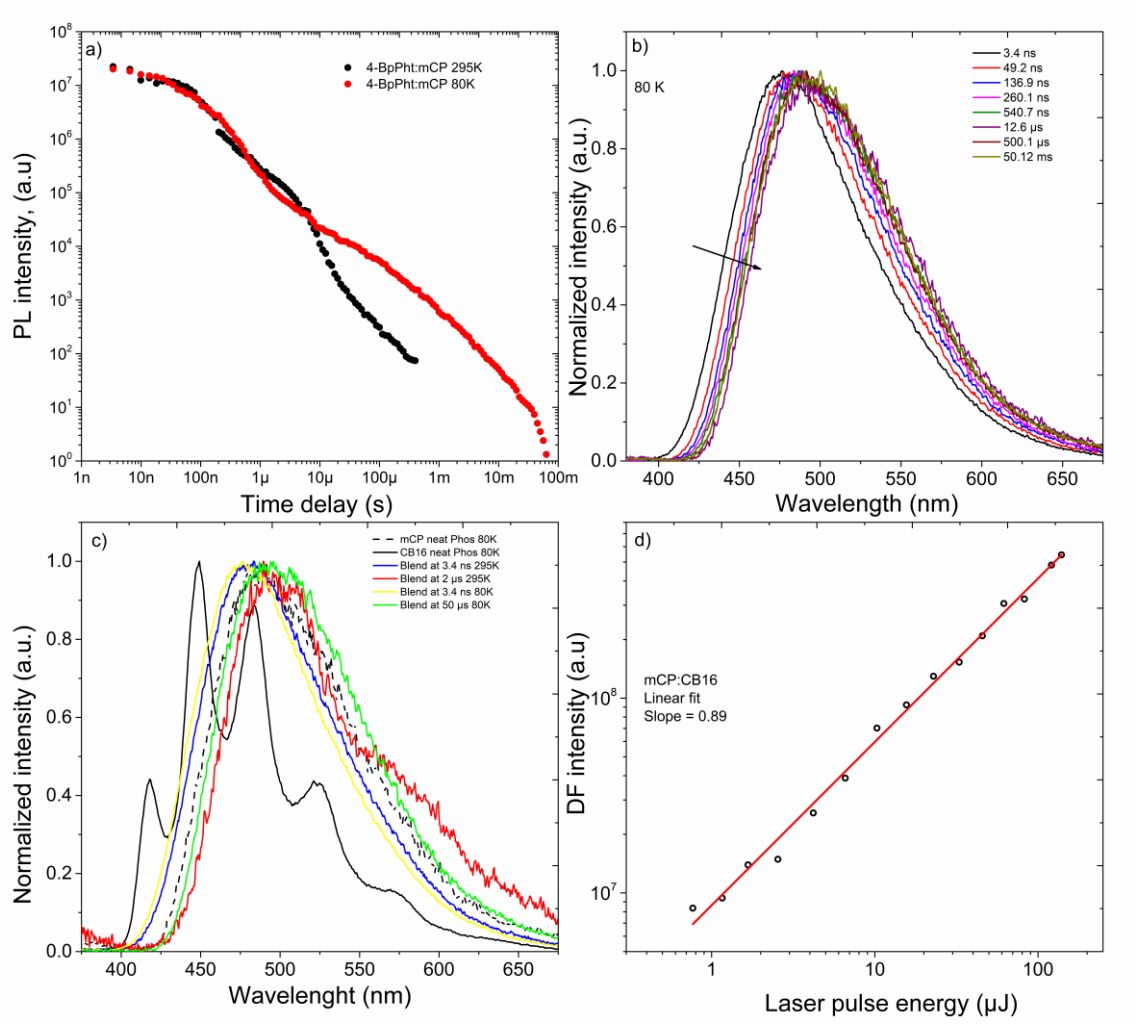

Figure 8. Time-resolved fluorescence decay curves of the layer of mCP:**4-BpPht** blend recorded at 295K and 80K (a). Time-resolved normalized emission spectra recorded at 80K (b). Prompt and delayed fluorescence spectra of exciplex-forming blend mCP:**4-BpPht** recorded at 295 K and 80 K and phosphorescence spectra of donor and acceptor (c). Laser power dependence of delayed fluorescence of mCP:**4-BpPht** recorded at room temperature (d).

Figure 8b shows the time-resolved photoluminescence spectra of mCP:**4-BpPht** at 80K. At the short delay time (3.4ns) the ^{1}CT state emission with a maximum peak at 475 nm was detected. With the increase of delay time, a redshift of the ^{1}CT emission band was observed up to 495 nm at a delay time of 12.6 µs. The further increase of delay time did not affect the ^{1}CT band. At low temperature, the ^{1}CT-^{3}CT states live longer due to the slower RISC. Concerning time-resolved emission spectra recorded at 295K (**Figure S15**) the similar

behavior of ^{1}CT relaxation was observed but with stronger redshift. This observation can be explained by the more efficient relaxation of the ^{1}CT at room temperature due to the increased vibrational energy.

From the energy of onset of prompt fluorescence of mCP:**4-BpPht** at 295K (**Figure 8c**) it is possible to determine the ^{1}CT energy level, which was found to be 2.98± 0.02eV. From the phosphorescence spectra of the donor and acceptor molecules shown in the Figure 8c the energies of locally excited state of the donor (^3LE_D) and locally excited state of the acceptor (^3LE_A) were determined as 2.92±0.02eV and 3.08± 0.02eV, respectively. In our system, ^3LE_A is above ^{1}CT, but ^3LE_D is located close to the ^{1}CT state (**Figure 8c**). In such situation, ^{1}CT can be in resonance with ^3LE_D, which allows spin-orbit coupling interaction of these states. This case of triplet harvesting is in good agreement with exciplexes that reported earlier[46]. The singlet-triplet splitting could be calculated as a difference between CT energy and ^3LE_D energy and was found to be of 0.06±0.03eV. It is worth to note that at long delay time (ms range) at 80K, in the spectrum of the blend also the phosphorescence of mCP could be observed, as a result of the significant singlet-triplet gap. In addition, the exciplex-forming molecular mixture at 80K showed enhanced prompt and delayed emission in comparison with the signals observed at 295 K. This observation can be explained by a high contribution of non-radiative transitions from singlet and triplet states[45].

To sum up, sky-blue mCP:**4-BpPht** exciplex-forming blend showed singlet-triplet splitting around 0.06±0.03eV and 26% of PLQY as a result of the decreased contribution of TADF in exciplex blend.

3.6. Device fabrication.

Since the layers of mCP:**4-BpPht** showed the highest PLQY value, this blend was used as an emitter to fabricate OLEDs. The device structure was as follows: ITO/ (NPB)(20nm)/ TCTA(10nm)/ mCP(5nm)/ mCP:**4-BpPht**(20nm)/ TmPyPB(50nm)/ LiF(1nm)/ Al(100nm). A thin layer of mCP was introduced into the device to prevent lower energy exciplex formation between TCTA and **4-BpPht** and triplet exciton quenching[47]. An emitting layer has been formed with weight ratio 1:1 by co-deposition of donor (mCP) and acceptor (**4-BpPht**) at the identical rate [48]. A 50 nm thick layer of TmPyPB was used as an ETL layer to improve electron transport since TmPyPB shows high electron mobility[49].

The exemplary output characteristics of OLED are presented in **Figure 9**; the energy levels diagram of the device is presented in **Figure 9c**. The wavelength of maximum intensity of electroluminescence (EL) spectrum of the device is almost the same as that of PL spectrum of molecular mixture mCP:**4-BpPht** (**Figure 9a**). Commission Internationale de l'Eclairage (CIE 1931) chromaticity coordinates (x, y) of OLED were determined as (0.24;0.41). Sky-blue OLED showed a turn-on voltage of 5 V (V_{on}) and maximum brightness (L_{max}) of 2500 cd m^{-2} at 12 V (Figure 9b). Maximum EQE ($\eta_{ext,max}$), power ($\eta_{P,max}$) and current efficiencies ($\eta_{L,max}$) were found to be 2.9%, 2.2 Lm W^{-1} and 4.9 cd A^{-1} respectively.

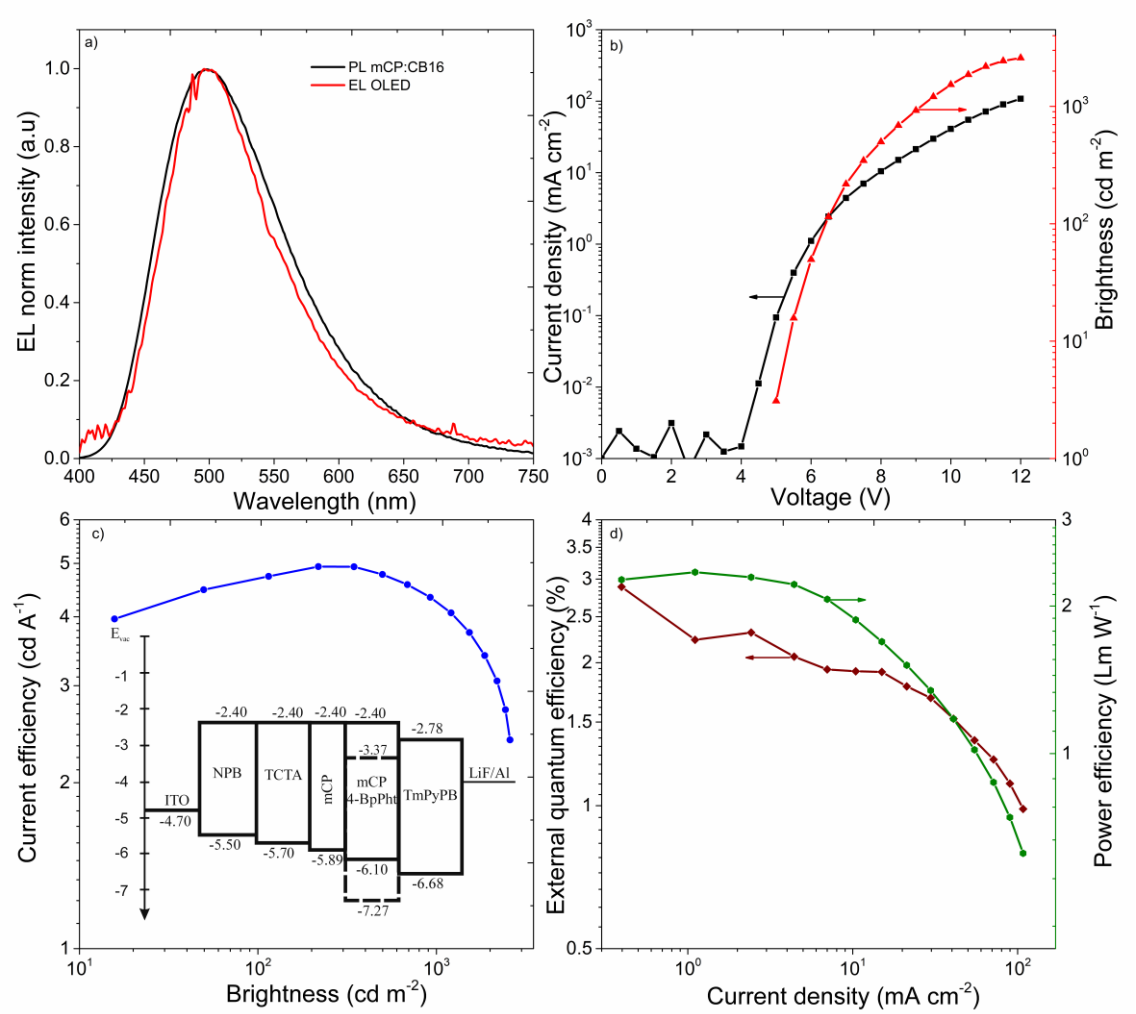

Figure 9. EL spectra of OLED and PL spectra of mCP:4-BpPht blend (a), Current density−voltage and luminance−voltage characteristics (b), current efficiency(energy band diagram of OLED) (c), power efficiency and quantum efficiency of the device based on CB16:mCP exciplex (d).

In addition, the maximum theoretical external quantum efficiency of the fabricated device based on the exciplex-forming light-emitting layer of mCP:**4-BpPht** was analyzed using the equation[50]:

$$\eta_{ext}=\gamma\times\phi_{PL}\times\chi\times\eta_{out} \qquad \text{(Eq. 1)}$$

where γ corresponds to the charge-balance factor, ϕ_{PL} is the photoluminescence quantum efficiency (ϕ_{PL}=0.26 for the mCP:**4-BpPht**), χ is the efficiency of exciton production (χ=0.25 or χ=1 in case of the fluorescence or TADF type devices, respectively), and η_{out} corresponds to the outcoupling efficiency (η_{out} is usually from 0.2 to 0.3). Assuming γ=1, χ=0.25 (in case of only singlet exciton utilization) and η_{out} =0.3, the maximum theoretical external quantum efficiency for the fabricated device is only 1.95 % as PLQY of 26 % was obtained for the solid layer of mCP:**4-BpPh**. Since the experimentally obtained max. external quantum efficiency is much higher - 2.9 % - utilization of both singlet and triplet excitons in electroluminescence of the studied device is clearly demonstrated. We have to note, however,

that the maximum theoretical external quantum efficiency for the fabricated device is 7.8 % assuming γ=1, χ=1 (in case of the singlet and triplet exciton utilization) and η_{out} =0.3. This maximum theoretical EQE is much higher than the experimental one. The efficiency of this OLED can be limited due to significant singlet-triplet energy gap and increased amount of non-radioactive losses in exciplex. We demonstrated the potential of phthalimide based derivatives as exciplex-forming materials for efficient devices exploiting utilization of both singlet and triplet excitons.

4. Conclusions

Synthesis and characterization of five phthalimide derivatives are reported. For the first time, exciplex forming properties of phthalimides based acceptors were described with carbazole containing donors. The difference in the molecular architecture of molecules did not effect for values of electron affinity and triplet levels but had an influence on exciplex forming properties. The compounds showed high triplet levels (2.92-3.11 eV) and similar electron affinities (3.3-3.4 eV). Phthalimide derivatives were suitable to achieve multicolor exciplex emission with carbazole containing donors, which covered a large part of the visible spectrum from sky-blue to orange colors. On the basis of photophysical investigation best performance showed phthalimide-benzophenone acceptors rather than two phthalimide moieties containing acceptors. Exciplxes containing non-symmetric phthalimide-benzophenone acceptors showed highest photoluminescence quantum yield in the solid state in comparison with symmetric phthalimide derivatives. The main reason is intramolecular charge transfer state which is indicated by the broad non-structured phosphorescence spectra of these materials and lower value of triplet levels. A para- substituted phthalimide-benzophenone (**4-BpPht**) showed better exciplex-forming properties in comparison to other materials and in the mixture with mCP exhibited sky blue exciplex emission with the highest among studied systems photoluminescence quantum yield of 26%. From time-resolved PL measurements at 80K and 295K a singlet-triplet energy splitting of 0.06±0.03eV was determined. OLED based on this emitting system showed the maximum external quantum efficiency of 2.9% and brightness of 2500 cd m^{-2} at 12V with triplet harvesting.

5. Notes

The authors declare no competing financial interest.

Acknowledgements
The authors would like to acknowledge the EXCILIGHT project funded by the European Union's Horizon 2020 Research and Innovation Programme under grant agreement No. 674990. This work was also supported by Research Council of Lithuania (Project "OWEX" No S-MIP-17-101). Special acknowledgement to prof. Tadeusz Biela for mass spectrometry analysis.

Appendix A. Supplementary material

Supplementary data associated with this article can be found, in the online version, at https://doi.org/10.1016/j.dyepig.XXXX.

References

[1] T. Hatakeyama, K. Shiren, K. Nakajima, S. Nomura, S. Nakatsuka, K. Kinoshita, J. Ni, Y. Ono, T. Ikuta, Ultrapure Blue Thermally Activated Delayed Fluorescence Molecules: Efficient HOMO-LUMO Separation by the Multiple Resonance Effect, Adv. Mater. 28 (2016) 2777–2781. doi:10.1002/adma.201505491.

[2] S. Reineke, F. Lindner, G. Schwartz, N. Seidler, K. Walzer, B. Lüssem, K. Leo, White organic light-emitting diodes with fluorescent tube efficiency, Nature. 459 (2009) 234–238. doi:10.1038/nature08003.

[3] H. Uoyama, K. Goushi, K. Shizu, H. Nomura, C. Adachi, Highly efficient organic light-emitting diodes from delayed fluorescence, Nature. 492 (2012) 234–238. doi:10.1038/nature11687.

[4] M.Y. Wong, E. Zysman-Colman, Purely Organic Thermally Activated Delayed Fluorescence Materials for Organic Light-Emitting Diodes, Adv. Mater. 29 (2017) 1605444. doi:10.1002/adma.201605444.

[5] T.-L. Wu, M.-J. Huang, C.-C. Lin, P.-Y. Huang, T.-Y. Chou, R.-W. Chen-Cheng, H.-W. Lin, R.-S. Liu, C.-H. Cheng, Diboron compound-based organic light-emitting diodes with high efficiency and reduced efficiency roll-off, Nat. Photonics. 12 (2018) 235–240. doi:10.1038/s41566-018-0112-9.

[6] K. Goushi, K. Yoshida, K. Sato, C. Adachi, Organic light-emitting diodes employing efficient reverse intersystem crossing for triplet-to-singlet state conversion, Nat. Photonics. 6 (2012) 253–258. doi:10.1038/nphoton.2012.31.

[7] M. Sarma, K.-T. Wong, Exciplex: An Intermolecular Charge-Transfer Approach for TADF, ACS Appl. Mater. Interfaces. 10 (2018) 19279–19304. doi:10.1021/acsami.7b18318.

[8] M. Cocchi, D. Virgili, C. Sabatini, J. Kalinowski, Organic electroluminescence from singlet and triplet exciplexes: Exciplex electrophosphorescent diode, Chem. Phys. Lett. 421 (2006) 351–355. doi:10.1016/j.cplett.2006.01.082.

[9] D. Graves, V. Jankus, F.B. Dias, A. Monkman, Photophysical Investigation of the Thermally Activated Delayed Emission from Films of m-MTDATA:PBD Exciplex, Adv. Funct. Mater. 24 (2014) 2343–2351. doi:10.1002/adfm.201303389.

[10] W.-Y. Hung, G.-C. Fang, S.-W. Lin, S.-H. Cheng, K.-T. Wong, T.-Y. Kuo, P.-T. Chou, The First Tandem, All-exciplex-based WOLED, Sci. Rep. 4 (2015) 5161. doi:10.1038/srep05161.

[11] M. Chapran, E. Angioni, N.J. Findlay, B. Breig, V. Cherpak, P. Stakhira, T. Tuttle, D. Volyniuk, J. V. Grazulevicius, Y.A. Nastishin, O.D. Lavrentovich, P.J. Skabara, An Ambipolar BODIPY Derivative for a White Exciplex OLED and Cholesteric Liquid Crystal Laser toward Multifunctional Devices, ACS Appl. Mater. Interfaces. 9 (2017) 4750–4757. doi:10.1021/acsami.6b13689.

[12] V. Cherpak, P. Stakhira, B. Minaev, G. Baryshnikov, E. Stromylo, I. Helzhynskyy, M. Chapran, D. Volyniuk, D. Tomkuté-Lukšienė, T. Malinauskas, V. Getautis, A. Tomkeviciene, J. Simokaitiene, J.V. Grazulevicius, Efficient "Warm-White" OLEDs Based on the Phosphorescent bis-Cyclometalated iridium(III) Complex, J. Phys. Chem. C. 118 (2014) 11271–11278. doi:10.1021/jp503437b.

[13] X.-K. Liu, Z. Chen, J. Qing, W.-J. Zhang, B. Wu, H.L. Tam, F. Zhu, X.-H. Zhang, C.-S. Lee, Remanagement of Singlet and Triplet Excitons in Single-Emissive-Layer Hybrid White Organic Light-Emitting Devices Using Thermally Activated Delayed Fluorescent Blue Exciplex, Adv. Mater. 27 (2015) 7079–7085. doi:10.1002/adma.201502897.

[14] J.-H. Lee, H. Shin, J.-M. Kim, K.-H. Kim, J.-J. Kim, Exciplex-Forming Co-Host-Based Red Phosphorescent Organic Light-Emitting Diodes with Long Operational Stability and High Efficiency, ACS Appl. Mater. Interfaces. 9 (2017) 3277–3281. doi:10.1021/acsami.6b14438.

[15] M.K. Etherington, F. Franchello, J. Gibson, T. Northey, J. Santos, J.S. Ward, H.F. Higginbotham, P. Data, A. Kurowska, P.L. Dos Santos, D.R. Graves, A.S. Batsanov, F.B.

Dias, M.R. Bryce, T.J. Penfold, A.P. Monkman, Regio- and conformational isomerization critical to design of efficient thermally-activated delayed fluorescence emitters, Nat. Commun. 8 (2017) 14987. doi:10.1038/ncomms14987.
[16] V. Jankus, P. Data, D. Graves, C. McGuinness, J. Santos, M.R. Bryce, F.B. Dias, A.P. Monkman, Highly Efficient TADF OLEDs: How the Emitter-Host Interaction Controls Both the Excited State Species and Electrical Properties of the Devices to Achieve Near 100% Triplet Harvesting and High Efficiency, Adv. Funct. Mater. 24 (2014) 6178–6186. doi:10.1002/adfm.201400948.
[17] F.B. Dias, J. Santos, D.R. Graves, P. Data, R.S. Nobuyasu, M.A. Fox, A.S. Batsanov, T. Palmeira, M.N. Berberan-Santos, M.R. Bryce, A.P. Monkman, The Role of Local Triplet Excited States and D-A Relative Orientation in Thermally Activated Delayed Fluorescence: Photophysics and Devices, Adv. Sci. 3 (2016) 1600080. doi:10.1002/advs.201600080.
[18] X. Yang, X. Xu, G. Zhou, Recent advances of the emitters for high performance deep-blue organic light-emitting diodes, J. Mater. Chem. C. 3 (2015) 913–944. doi:10.1039/C4TC02474E.
[19] Y. Tao, C. Yang, J. Qin, Organic host materials for phosphorescent organic light-emitting diodes, Chem. Soc. Rev. 40 (2011) 2943. doi:10.1039/c0cs00160k.
[20] J. Yu, J. Yang, X. Zhou, S. Yu, Y. Tang, H. Wang, J. Chen, S. Zhang, X. Guo, Phthalimide-Based Wide Bandgap Donor Polymers for Efficient Non-Fullerene Solar Cells, Macromolecules. 50 (2017) 8928–8937. doi:10.1021/acs.macromol.7b01958.
[21] H. Xin, X. Guo, F.S. Kim, G. Ren, M.D. Watson, S.A. Jenekhe, Efficient solar cells based on a new phthalimide-based donor–acceptor copolymer semiconductor: morphology, charge-transport, and photovoltaic properties, J. Mater. Chem. 19 (2009) 5303. doi:10.1039/b900073a.
[22] G. Zhang, J. Guo, J. Zhang, P. Li, J. Ma, X. Wang, H. Lu, L. Qiu, A phthalimide- and diketopyrrolopyrrole-based A 1 –π–A 2 conjugated polymer for high-performance organic thin-film transistors, Polym. Chem. 6 (2015) 418–425. doi:10.1039/C4PY00916A.
[23] S.-H. Lee, D. Khim, Y. Xu, J. Kim, W.-T. Park, D.-Y. Kim, Y.-Y. Noh, Simultaneous Improvement of Hole and Electron Injection in Organic Field-effect Transistors by Conjugated Polymer-wrapped Carbon Nanotube Interlayers, Sci. Rep. 5 (2015) 10407. doi:10.1038/srep10407.
[24] F. Dumur, M. Ibrahim-Ouali, D. Gigmes, Organic Light-Emitting Diodes Based on Phthalimide Derivatives: Improvement of the Electroluminescence Properties, Appl. Sci. 8 (2018) 539. doi:10.3390/app8040539.
[25] M.E. Jang, T. Yasuda, J. Lee, S.Y. Lee, C. Adachi, Organic Light-emitting Diodes Based on Donor-substituted Phthalimide and Maleimide Fluorophores, Chem. Lett. 44 (2015) 1248–1250. doi:10.1246/cl.150454.
[26] S. Srinivas, F.E. Caputo, M. Graham, S. Gardner, R.M. Davis, J.E. McGrath, G.L. Wilkes, Semicrystalline Polyimides Based on Controlled Molecular Weight Phthalimide End-Capped 1,3-Bis(4-aminophenoxy)benzene and 3,3‘,4,4‘-Biphenyltetracarboxylic Dianhydride: Synthesis, Crystallization, Melting, and Thermal Stability, Macromolecules. 30 (1997) 1012–1022. doi:10.1021/ma9604597.
[27] M. Li, S.-H. Li, D. Zhang, M. Cai, L. Duan, M.-K. Fung, C.-F. Chen, Stable Enantiomers Displaying Thermally Activated Delayed Fluorescence: Efficient OLEDs with Circularly Polarized Electroluminescence, Angew. Chemie Int. Ed. 57 (2018) 2889–2893. doi:10.1002/anie.201800198.
[28] N. Venkatramaiah, G.D. Kumar, Y. Chandrasekaran, R. Ganduri, S. Patil, Efficient Blue and Yellow Organic Light-Emitting Diodes Enabled by Aggregation-Induced Emission, ACS Appl. Mater. Interfaces. 10 (2018) 3838–3847. doi:10.1021/acsami.7b11025.
[29] M. Li, Y. Liu, R. Duan, X. Wei, Y. Yi, Y. Wang, C.-F. Chen, Aromatic-Imide-Based Thermally Activated Delayed Fluorescence Materials for Highly Efficient Organic Light-Emitting Diodes, Angew. Chemie Int. Ed. 56 (2017) 8818–8822. doi:10.1002/anie.201704435.
[30] J.M. Chapman, P.J. Voorstad, G.H. Cocolas, I.H. Hall, Hypolipidemic activity of phthalimide derivatives. 2. N-Phenylphthalimide and derivatives, J. Med. Chem. 26 (1983) 237–243. doi:10.1021/jm00356a022.

[31] C.M. Cardona, W. Li, A.E. Kaifer, D. Stockdale, G.C. Bazan, Electrochemical Considerations for Determining Absolute Frontier Orbital Energy Levels of Conjugated Polymers for Solar Cell Applications, Adv. Mater. 23 (2011) 2367–2371. doi:10.1002/adma.201004554.
[32] P. Data, P. Pander, M. Lapkowski, A. Swist, J. Soloducho, R.R. Reghu, J.V. Grazulevicius, Unusual properties of electropolymerized 2,7- and 3,6- carbazole derivatives, Electrochim. Acta. 128 (2014) 430–438. doi:10.1016/j.electacta.2013.12.108.
[33] M.J. Frisch, G.W. Trucks, H.B. Schlegel, G.E. Scuseria, M.A. Robb, J.R. Cheeseman, G. Scalmani, V. Barone, B. Mennucci, G.A. Petersson, H. Nakatsuji, M. Caricato, X. Li, H.P. Hratchian, A.F. Izmaylov, J. Bloino, G. Zheng, J.L. Sonnenberg, M. Hada, M. Ehara, K. Toyota, R. Fukuda, J. Hasegawa, M. Ishida, T. Nakajima, Y. Honda, O. Kitao, H. Nakai, T. Vreven, J.A. Montgomery Jr., J.E. Peralta, F. Ogliaro, M. Bearpark, J.J. Heyd, E. Brothers, K.N. Kudin, V.N. Staroverov, R. Kobayashi, J. Normand, K. Raghavachari, A. Rendell, J.C. Burant, S.S. Iyengar, J. Tomasi, M. Cossi, N. Rega, J.M. Millam, M. Klene, J.E. Knox, J.B. Cross, V. Bakken, C. Adamo, J. Jaramillo, R. Gomperts, R.E. Stratmann, O. Yazyev, A.J. Austin, R. Cammi, C. Pomelli, J.W. Ochterski, R.L. Martin, K. Morokuma, V.G. Zakrzewski, G.A. Voth, P. Salvador, J.J. Dannenberg, S. Dapprich, A.D. Daniels, O. Farkas, J.B. Foresman, J. V Ortiz, J. Cioslowski, D.J. Fox, Gaussian 09, Revision A.02 Wallingford, CT, 2009.
[34] J. Gawronski, F. Kazmierczak, K. Gawronska, U. Rychlewska, B. Nordén, A. Holmén, Excited States of the Phthalimide Chromophore and Their Exciton Couplings: A Tool for Stereochemical Assignments, J. Am. Chem. Soc. 120 (1998) 12083–12091. doi:10.1021/ja982131u.
[35] J.R. Lakowicz, ed., Principles of Fluorescence Spectroscopy, Springer US, Boston, MA, 2006. doi:10.1007/978-0-387-46312-4.
[36] P.H. Pander, S. Gogoc, M. Colella, P. Data, F.B. Dias, Thermally-Activated Delayed Fluorescence in Polymer-Small Molecule Exciplex Blends for Solution-Processed Organic Light-Emitting Diodes, ACS Appl. Mater. Interfaces. (2018) 10, 28796–28802. doi:10.1021/acsami.8b07554.
[37] W. Liu, J.-X. Chen, C.-J. Zheng, K. Wang, D.-Y. Chen, F. Li, Y.-P. Dong, C.-S. Lee, X.-M. Ou, X.-H. Zhang, Novel Strategy to Develop Exciplex Emitters for High-Performance OLEDs by Employing Thermally Activated Delayed Fluorescence Materials, Adv. Funct. Mater. 26 (2016) 2002–2008. doi:10.1002/adfm.201505014.
[38] K.-H. Kim, S.-J. Yoo, J.-J. Kim, Boosting Triplet Harvest by Reducing Nonradiative Transition of Exciplex toward Fluorescent Organic Light-Emitting Diodes with 100% Internal Quantum Efficiency, Chem. Mater. 28 (2016) 1936–1941. doi:10.1021/acs.chemmater.6b00478.
[39] N.G. Tsierkezos, Investigation of the Electrochemical Reduction of Benzophenone in Aprotic Solvents Using the Method of Cyclic Voltammetry, J. Solution Chem. 36 (2007) 1301–1310. doi:10.1007/s10953-007-9188-4.
[40] H.A. Zamani, PVC-Membrane Potentiometric Electrochemical Sensor Based on 2-(4-Oxopentan-2-ylideneamino)isoindoline-1,3-dione for Selective Determination of Holmium(III), E-Journal Chem. 8 (2011) S97–S104. doi:10.1155/2011/158389.
[41] J. Kalinowski, M. Cocchi, D. Virgili, V. Fattori, J.A.G. Williams, Mixing of Excimer and Exciplex Emission: A New Way to Improve White Light Emitting Organic Electrophosphorescent Diodes, Adv. Mater. 19 (2007) 4000–4005. doi:10.1002/adma.200700655.
[42] M. Gordon, W.R. Ware, eds., The Exciplex, Academic Press, 1975.
[43] J. Kalinowski, Excimers and exciplexes in organic electroluminescence, Mater. Sci. 27 (2009) 735–756. doi:10.1038/2141187a0.
[44] P. Pander, A. Kudelko, A. Brzeczek, M. Wroblowska, K. Walczak, P. Data, Analysis of Exciplex Emitters, Disp. Imaging. 2 (2017) 265–277.
[45] F.B. Dias, Kinetics of thermal-assisted delayed fluorescence in blue organic emitters with large singlet-triplet energy gap, Philos. Trans. R. Soc. A Math. Phys. Eng. Sci. 373 (2015) 20140447–20140447. doi:10.1098/rsta.2014.0447.

[46] P.L. dos Santos, F.B. Dias, A.P. Monkman, Investigation of the Mechanisms Giving Rise to TADF in Exciplex States, J. Phys. Chem. C. 120 (2016) 18259–18267. doi:10.1021/acs.jpcc.6b05198.
[47] Y. Seino, S. Inomata, H. Sasabe, Y.-J. Pu, J. Kido, High-Performance Green OLEDs Using Thermally Activated Delayed Fluorescence with a Power Efficiency of over 100 lm W −1, Adv. Mater. 28 (2016) 2638–2643. doi:10.1002/adma.201503782.
[48] W. Hung, T. Wang, P. Chiang, B. Peng, K. Wong, Remote Steric Effect as a Facile Strategy for Improving the Efficiency of Exciplex-Based OLEDs. ACS Appl. Mater. Interfaces 2017, 9, 7355–7361. doi: 10.1021/acsami.6b16083
[49] S.-J. Su, T. Chiba, T. Takeda, J. Kido, Pyridine-Containing Triphenylbenzene Derivatives with High Electron Mobility for Highly Efficient Phosphorescent OLEDs, Adv. Mater. 20 (2008) 2125–2130. doi:10.1002/adma.200701730.
[50] T. Tsutsui, Progress in Electroluminescent Devices Using Molecular Thin Films, MRS Bull. 22 (1997) 39–45. doi:10.1557/S0883769400033613.